Revealing the Limits of Intermolecular Interactions: Molecular Rings of Ferrocene Derivatives on Graphite Surface

Prithwidip Saha,[†] Vivek Kumar Yadav,[‡] Vinithra Gurunarayanan,[†] Ramesh Ramapanicker,[†] Jayant K. Singh,[‡] and Thiruvancheril G. Gopakumar*[,†]

[†]Department of Chemistry, Indian Institute of Technology Kanpur, Kanpur, Uttar Pradesh 208016, India
[‡]Department of Chemical Engineering, Indian Institute of Technology Kanpur, Kanpur, Uttar Pradesh 208016, India

S Supporting Information

ABSTRACT: We report the formation of discrete molecular rings/spirals of small molecules (1,3-dithia derivatives of ferrocene) on a highly oriented pyrolytic graphite (HOPG) surface. On the basis of microscopy and theoretical calculations, molecular level arrangement within the molecular rings is understood. The molecular rings show a limiting inner diameter, and we interpret it to be related to the critical intermolecular interaction limit. This limiting value of the inner diameter is surprisingly correlated with that observed for molecular rings/disks of a few reported molecules. The correlation reveals that molecular rings formed typically by weak van der Waals interactions should always show a limiting inner diameter and should be independent of molecular structure, size, and chemical nature.
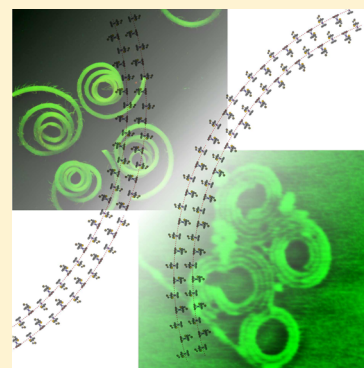
Discrete spherical/porous structures of macro/large biomolecules are commonly observed in nature,[1,2] which are stabilized by the interplay of enormous inter- and intramolecular interactions within them. However, such structures are not very commonly observed when small molecules (compared to macro/large biomolecules) assemble on surfaces. On the other hand, porous network patterns stabilized by strong hydrogen bonding have been reported for small molecules on surfaces.[3−7] Self-assembly of molecules based on weak van der Waals interactions typically shows dense packed molecular patterns on the surface;[8,9] however, porous network patterns are observed when long alkyl side chains are present in the molecules.[10−13] Both porous and dense packed two-dimensional (2D) molecular patterns have definite unit building cells. On the contrary, structures like discrete rings of molecules cannot be constructed using definite building unit cells as in 2D molecular patterns. Therefore, the formation of molecular rings is not often controllable in self-assembly on surfaces and is observed serendipitously.

So far, only a few spontaneous formations of discrete molecular rings (molecules as building blocks) have been reported. Molecular rings/spirals have been shown for alkyl-substituted tetrathiafulvalene[14] and long-chain carboxylic acids[15] on a HOPG surface. However, strong molecule−substrate (metallic) interactions[16−18] and templates like gas bubbles[19−21] have shown to trigger the formation of molecular rings on different surfaces. The spontaneously formed discrete molecular rings reported so far are based on large molecules with high structural flexibility. This suggests that the large size and structural flexibility possibly offer multitudes of weak interactions and diverse geometries for the molecule to form discrete rings. Such rings are scarce on surfaces possibly due to the requirement of several conditions like suitable molecular geometry, the interplay of intermolecular and molecule−surface interactions, suitable thermodynamical factors, etc. to be satisfied.

In this Letter, we report the serendipitous observation of molecular rings/spirals in the ultrathin film of 2-ferrocenyl-1,3-dithiane (Figure 1a, FcS_2C_4) and 2-ferrocenyl-1,3-dithiolane
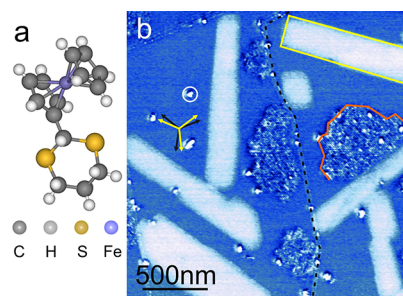

Figure 1. (a) Structure of FcS_2C_4 as obtained from X-ray crystal data. (b) AFM phase image of an ultrathin film of FcS_2C_4 on a HOPG (0001) surface. Yellow and orange lines depict 1D and 2D islands, respectively. Orientations of 1D islands (long edge) are marked by yellow and black arrows. A terrace edge is marked with a dashed black line.

(Figure 3a, FcS_2C_3) at the HOPG−air interface. These Fc derivatives are the smallest and most rigid known molecules, forming discrete molecular rings on the surface stabilized particularly by weak van der Waals interaction. Our observation in comparison with the literature suggests that the limiting inner diameter of molecular rings/spirals is related to the critical interaction limit of molecules within the rings/spirals and is independent of molecular geometry, size, and chemical nature.

Figure 1b shows a typical AFM phase image of an ultrathin film of FcS_2C_4 prepared at the HOPG−air interface by drop-casting from methanolic solution at ambient conditions. Further experimental details are provided in the SI. Two types of molecular domains are observed: One dimensional island (1D island, marked with yellow line) and Two dimensional island (2D island, marked with an orange line). The microscopic structure of these growths has been well understood in our previous report.[22] The relative percentage of 1D islands (∼65%) is higher with respect to that of 2D islands.

Upon annealing the above ultrathin film, striking changes are observed in its morphology. Figure 2a,b shows typical AFM
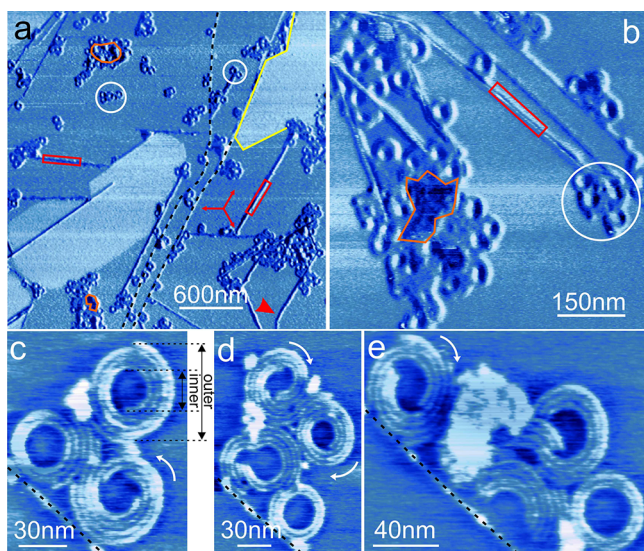

Figure 2. (a,b) AFM phase images of an ultrathin film of FcS_2C_4 on a HOPG(0001) surface after annealing at ∼353 K. Yellow and orange lines depict 1D islands and 2D islands, respectively. Parts of 1D chains and molecular rings/spirals are marked by red lines and white circles, respectively. Red arrows depict the orientations of 1D chains with respect to their length. The red arrowhead indicates a curved 1D chain. Terrace edges are indicated with black dashed lines. (c−e) High-resolution AFM phase images of molecular rings. Directions of coiling within the spirals are indicated with white curved arrows.

phase images of an ultrathin film of FcS_2C_4 annealed at ∼353 K (corresponding topographs are provided in the SI). 1D islands (yellow lines) coalesce to larger domains, yet the orientation and well-defined growth facets are preserved. The total coverage of 2D islands decreases drastically, and they appear as small domains (marked with orange lines). In addition, long chain-like structures (red lines) and rings (white circles) are observed. We address these chains as 1D chains owing to the nature of the growth. Typically the 1D chains grow as long as several μm, and their growth is limited only by other molecular domains on the surface. Three typical orientations (red arrows in Figure 2a) suggest that the 1D

chains are aligned to the graphite compact lattice directions (see additional images in the SI for the same). Further high-resolution images of molecular rings (Figure 2c−e) reveal the following. Molecular rings are either concentric or spirals with a minimum of two circles (we did not observe molecular rings with one circle). The spirals are coiled either clockwise or counterclockwise (indicated by curved arrows). There is a limiting value of outer and inner diameter (indicated in Figure 2c using double headed arrows) for the molecular rings, 44 ± 4 and 22 ± 3 nm, respectively. Molecular ring pairs formed by clockwise and counterclockwise spirals are also seldom observed (cf. Figure 2c).

We note that the molecular rings/spirals are observed between 353 and 393 K; above 393 K, we observe that the molecular rings break, as observed by the abundance of half-rings (see AFM images in the SI). 1D chains, molecular rings, and 1D islands desorb when the film is annealed above 393 K and completely desorb at 413 K. We observe that as the temperature increases the absolute coverage of 1D chains and molecular rings/spirals decreases marginally. Absolute coverage varies between samples (depends on the concentration of the drop-casting solution), and therefore, we use a single sample preparation for the percentage analysis. The absolute coverages of 1D chains and molecular rings are 7.6 and 6.7% at 353 K, 7.0 and 7.6% at 373 K, and 5.0 and 5.6% at 393 K, respectively. However, the absolute coverage of 2D islands decreases drastically (6.9% at 353 K, 5.0% at 373 K, and 2.0% at 393 K) with temperature. Because the change in percentage of 1D chains and molecular rings/spirals is comparable with increasing temperature, we presume that their relative stability is comparable. On a comparative scale, the stability of 2D islands with respect to others is very low.

We studied the ultrathin film of a slightly different ferrocene derivative (FcS_2C_3, Figure 3a) on HOPG. An "as-deposited" ultrathin film of FcS_2C_3 shows similar 1D and 2D islands as those observed in the case of FcS_2C_4 (see data in the SI).[22] Upon annealing this film (Figure 3b,c), we observe 1D chains (red lines) and molecular rings (white circles). The outer and inner diameters of the molecular rings show limiting values of 40 ± 4 and 20 ± 3 nm, respectively. These diameters are comparable to those of the molecular rings of FcS_2C_4. In addition, the 1D islands (yellow lines) coalesce into large domains; the abundance of 2D islands (orange lines) drastically decreases, and the remaining 2D islands are observed near molecular rings. We also observe a self-assembled hexagonal superlattice of molecular rings (possibly by discrete and or paired rings), as shown in Figures 3d and S6. Additional AFM images and details may be found in the SI. Similar as in FcS_2C_4, the molecular patterns of FcS_2C_3 completely desorb above 413 K.

Next, we discuss the microscopic arrangement of molecules in both 1D/2D islands, 1D chains, and molecular rings/spirals. The microscopic model for the arrangement of molecules in 1D/2D islands[22] and that in 1D chains[23] were reported previously. The molecules in 1D and 2D islands are stabilized by an edge-to-face ($-C-H\cdots\pi$) interaction.[22] The molecules in the 1D chain are stabilized through an edge-to-center ($-C-H\cdots$ metal) interaction.[23−26] These arrangements are also known in metallocene assemblies on surfaces.[25,27,28] Figure 4a shows the optimized geometry (using DFT implemented in Quantum ESPRESSO; see details in the SI) of molecular packing in a 1D chain of FcS_2C_4 on a bilayer graphite. The model for the 1D chain of FcS_2C_3 is provided in the SI. It is to
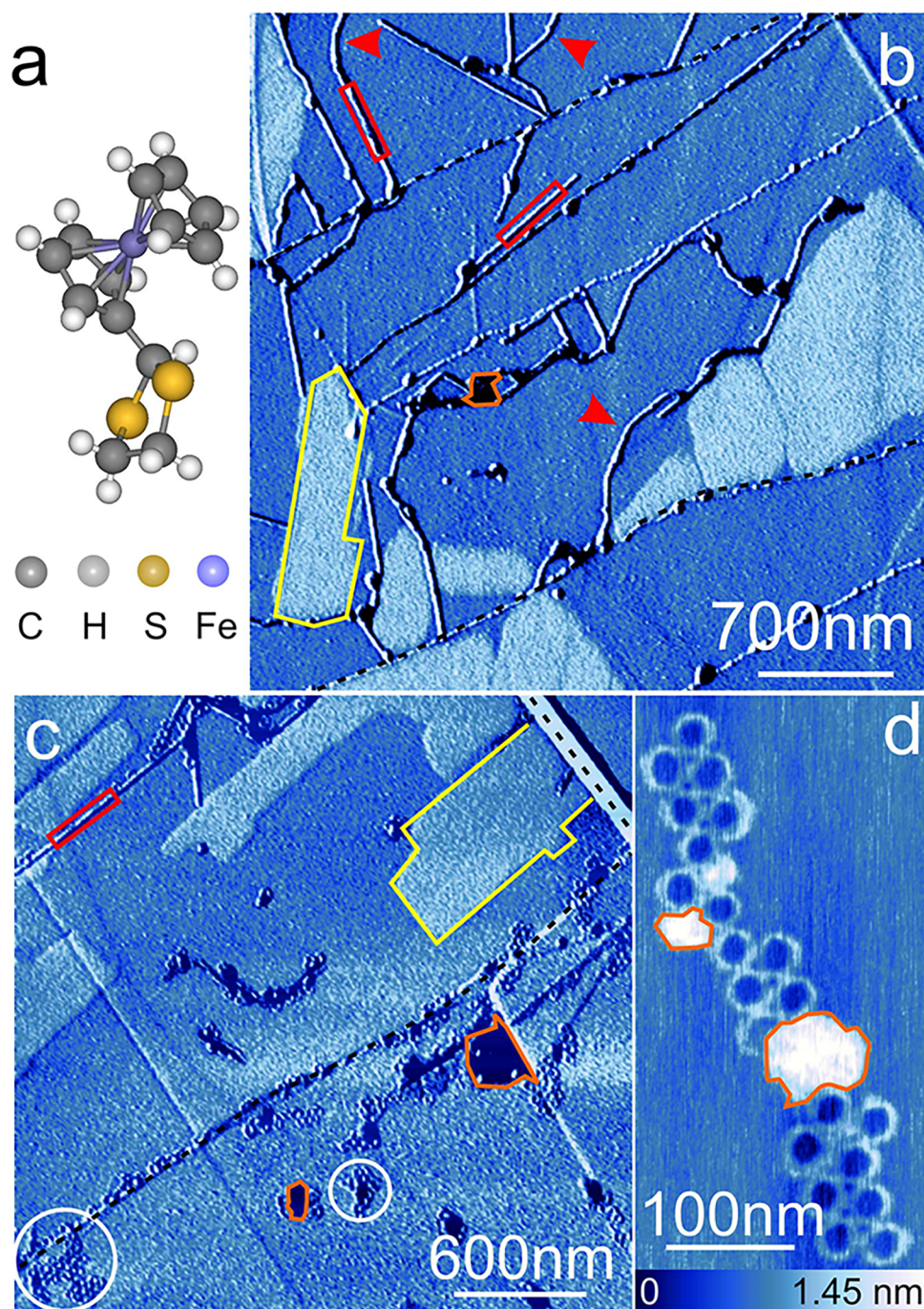
Figure 3. (a) Structure of FcS_2C_3 as obtained from X-ray crystal data. (b,c) AFM phase images of an ultrathin film of FcS_2C_3 on a HOPG(0001) surface after annealing at ~353 K. Yellow, orange, and red line and the white circle indicate coalesced 1D islands, 2D islands, 1D chains, and molecular rings, respectively. A few terrace edges are marked with black dashed lines. Red arrowheads indicate a few curved/bent 1D chains. (d) High-resolution AFM topograph of self-assembly of molecular rings.

be noted that along the length of the chain ($\vec{A}$), the adsorption geometry allows a T-shaped $\pi-\pi$ interaction between Cp rings and graphite.[28−30] This most likely favors the extended growth of the 1D chain along three typical directions on graphite, as observed experimentally.

We propose that the molecular rings/spirals have similar microscopic packing as in a 1D chain. We observed several 1D chains with curved/bent geometry for both molecules (images with short bent/curved 1D chains are provided in the SI and also indicated using red arrowheads in Figures 2a and 3b). Because curves are the building elements of rings, we propose

that molecular rings are formed upon coiling of 1D chains. The proposed microscopic packing of the curved 1D chain of FcS_2C_4 is shown in Figure 4b (the corresponding model for FcS_2C_3 is provided in the SI). The dimer building block (indicated using a dashed oval) is similar to that of the 1D chain. Curvature of the 1D chain is obtained by rotating the molecular axis (magenta lines) of adjacent molecules by 3 ± 0.1°. All adjacent molecules possess the same angle of rotation with respect to its neighbor, and thus, the curved 1D chain is propagated. The angle of rotation of molecules is chosen such that the radius of curvature of the ring (21.5 nm) corresponds
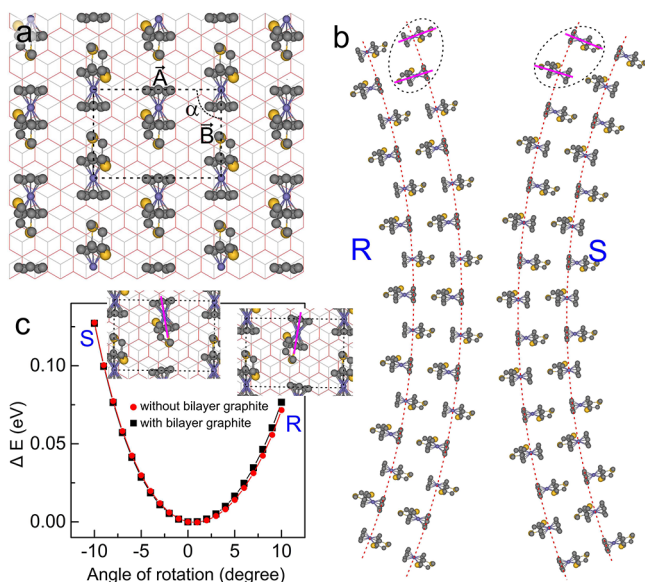
Figure 4. Optimized geometry corresponding to a 1D chain of FcS_2C_4 (a) on bilayer graphite. The unit cell is marked with a black dashed rectangle. $\vec{A}$ (1.22 nm) and $\vec{B}$ (0.85 nm) are the unit cell vectors, and α (90°) is the angle between them. (b) Proposed model for the curved 1D chain of FcS_2C_4. (c) Difference in total energy (ΔE) as a function of the angle of rotation of the molecular axis (magenta line) of the molecule at the center of the unit cell. R and S depict molecular rings constructed by R and S dimers, respectively.

to the limiting inner diameter of the molecular rings of FcS_2C_4. We propose that the limiting value of the inner diameter is most likely related to the maximum allowed rotation of adjacent molecules (with respect to the ideal dimer of the 1D chain) up to which the intermolecular interactions are energetically favorable at ambient conditions.

To understand this further, we performed a potential energy scan (PES) for the relative orientation of a molecule in the unit cell of a 1D chain (2 molecules per cell and with periodic boundary conditions on bilayer graphite; see details in the SI). One molecule in the unit cell (indicated with a magenta line in Figure 4c) is rotated with respect to its neighbors, and the total energy is calculated. Figure 4c shows the difference in the total energy (ΔE) of different configurations with respect to the energy of the unit cell of the 1D chain; a higher positive value indicates low relative stability. It is striking to note that ΔE is asymmetric around 0°. This suggests that a slightly rotated configuration of molecules within the unit cell is relatively stable compared to that in a 1D chain. The variation in ΔE for configurations within −5 and +5° is below the thermal energy at room temperature (RT), which suggests that such dimers are feasible at RT. Therefore, the ring formation with dimers having relatively rotated orientation within this range is energetically favorable at RT. The asymmetry in ΔE is attributed to the functional group that influences the interaction between the molecules (functional group breaks the symmetry of Fc). R depicts a dimer where the molecular axis of one molecule is rotated clockwise with respect to an ideal dimer, and S is the dimer with one molecule rotated counterclockwise. Figure 4b includes part of molecular rings constructed using R and S dimers. Depending on the relative orientation of molecules, clockwise and counterclockwise coiling or concentric molecular rings are feasible on graphite, as experimentally observed. The PES and the corresponding

models for molecular rings for FcS_2C_3 are shown in the SI, which also shows similar observations as FcS_2C_4. We also calculated the PES without bilayer graphite; surprisingly no major difference is observed compared to that with bilayer graphite. This indicates that the molecular rings are stabilized through molecule−molecule interactions and the substrate plays no major role. To further validate the asymmetry in ΔE, we compared the PES for the unit cell (same as that in Figure 4a) and a large unit cell (to mimic a situation of a dimer without neighbors) without graphite. See the SI for the results. It is observed that even for the dimer alone the asymmetry in the ΔE is substantial. This indicates that dimers of variable molecular orientations are expected on the surface and are the building blocks for the different types of molecular rings.

We propose two possible mechanisms for the formation of molecular rings/spirals: (a) condensation of molecules near bubbles of solvents and the kinetic trapping of molecules into ring structures and (b) molecules within the rings stabilized by a limiting intermolecular interaction at the given thermodynamical conditions. If molecules condense near solvent bubbles, one would expect variable sizes for the rings, as expected from the possible variety of sizes of bubbles. However, we observe a unique inner/outer diameter for the molecular rings (within experimental error). In addition, the minimum size (~20 nm) and the ordered assembling of rings at free terraces could not be explained using a solvent droplet drying mechanism. Previously reported molecular rings formed near bubbles show variable diameters.[19−21] We note that the molecular rings in our case are observed upon annealing the "as-deposited" film above the solvent boiling point. The percentage of molecular rings remains comparable in the temperature range between ~353 and ~393 K (see the percentage above). This further supports that the molecular rings are not formed by kinetic trapping around the solvent droplets (solvent is not expected at this temperature on the surface). Instead, they are thermodynamically stable structures stabilized by intermolecular interaction. We have shown above that the total energy (also related to the intermolecular interaction energy) is lowest when molecules orient asymmetric with respect to their neighboring molecules and molecule rings may be constructed with such orientation of neighboring molecules. Thus, we presume that the formation of molecular rings is thermodynamically driven and not kinetically. This also suggests that the observed limiting inner/outer diameter of molecular rings is related to the critical limit of intermolecular interactions between molecules (at given thermodynamic conditions) within the molecular rings. The intermolecular interaction within the rings is also not influenced by the surface, as revealed in the calculations. However, the atomically flat graphite surface should act as a template as the molecule−molecule interaction is strongly dependent on the relative adsorption geometry of neighboring molecules within the ring. We note that on a silicon surface (with roughness $\approx$ 1 nm) we observed only clusters of molecules at RT and also after annealing. The growth of 1D islands and 1D chains is epitaxially grown with respect to the substrate symmetry, as observed by the preferential 6-fold and 3-fold orientations, respectively.

We have shown previously that 1D islands are energetically favorable compared to 2D islands.[22,23] Upon annealing, the relative abundance of 2D islands (~35% at RT and ~11% at 353 K) diminishes drastically compared to 1D islands (~65% at RT and ~64% at 353 K). In addition, it is observed that the

remaining amount of 2D islands (indicated with orange lines; cf. Figures 2a,b and 3c,d) is always in the vicinity of 1D chains and molecular rings. This observation suggests tentatively that the 1D chains and molecular rings originate from energetically less stable 2D islands. To confirm this further, we prepared the ultrathin films of FcS_2C_4 and FcS_2C_3 on HOPG from ethanol. We had shown previously that when molecular ultrathin films of FcS_2C_4 and FcS_2C_3 are formed from ethanol, they exclusively form 1D islands, and no 2D islands are observed.[22] Further annealing of an ultrathin film of molecules prepared from ethanol reveals no 1D chains or molecular rings; only coalesced 1D islands are observed (AFM images are provided in the SI). This supports further that the 1D chains and molecular rings are thermodynamically favorable assemblies and originate from energetically less favorable 2D islands. As energetically less stable 2D islands are necessary for the formation of molecular rings, the solvent for the preparation of the ultrathin film also remains important.

We also find a surprising correlation in the inner/outer limiting diameters of the molecular rings of FcS_2C_4 and FcS_2C_3 with those of a few reported molecules.[14,15] See the comparison in the table provided in the SI. The biggest surprise here is whether the correlation is a mere coincidence or it suggests that the inner/outer diameter of molecular rings is independent of the molecular geometry and size. As revealed in the PES calculations, energetically favorable asymmetric molecular dimers are the key to the formation of molecular rings. Therefore, the limiting inner/outer diameter should be related to the limiting intermolecular interactions. We presume a similar scenario for the previously reported molecular rings/spirals.[14,15] Thus, it is summarized that molecular rings formed by predominantly weak intermolecular interactions should always possess a limiting inner/outer diameter and should be independent of size, shape, and chemical nature of the molecules. We also note that the molecular rings with a very small inner diameter (~4 nm) are possible if the formation of rings is assisted by a strong molecule−substrate interaction.[16,18]

We observe the formation of discrete molecular rings/spirals of two small ferrocene derivatives on graphite. The molecular rings show a limiting value of the inner and outer diameters, which closely correlates with those of molecular rings of a few other molecules on graphite. On the basis of the microscopic and theoretical analysis, we conclude that the formation of discrete molecular rings and the limiting inner/outer diameter are related to the critical intermolecular interaction at given thermodynamic conditions. Our analysis also suggests that discrete molecular rings are possible for any asymmetric molecule at suitable thermodynamic conditions (irrespective of their size) if the molecule−molecule interaction is dominantly weak interactions. Furthermore, molecules interacting through strong hydrogen bonding may not form discrete molecular rings due to the strength and directionality of the intermolecular interactions.

■ ASSOCIATED CONTENT

Ⓢ Supporting Information

The Supporting Information is available free of charge at https://pubs.acs.org/doi/10.1021/acs.jpclett.9b03357.

Experimental details; additional AFM topograph/phase image of molecular rings of FcS_2C_4; AFM study of an ultrathin film of FcS_2C_3; AFM phase images of an ultrathin film of FcS_2C_4 drop-casted from ethanol; details of the theoretical calculations; optimized geometry of the 1D chain and model for a molecular ring of FcS_2C_3; PES for different cell sizes; and diameter of molecular rings of different molecules (PDF)

■ AUTHOR INFORMATION

Corresponding Author
*E-mail: gopan@iitk.ac.in. Phone: +91 5122596830. Fax: +91 5122596806.

ORCID Ⓞ
Prithwidip Saha: 0000-0003-2600-0415
Vivek Kumar Yadav: 0000-0002-9142-4567
Ramesh Ramapanicker: 0000-0002-7717-6843
Jayant K. Singh: 0000-0001-8056-2115
Thiruvancheril G. Gopakumar: 0000-0002-3219-7907

Notes
The authors declare no competing financial interest.

■ REFERENCES

(1) Müller, D. J.; Sass, H.-J.; Müller, S. A.; Büldt, G.; Engel, A. Surface structures of native bacteriorhodopsin depend on the molecular packing arrangement in the membrane. *J. Mol. Biol.* **1999**, *285*, 1903.

(2) Bahatyrova, S.; Frese, R. N.; Siebert, C. A.; Olsen, J. D.; van der Werf, K. O.; van Grondelle, R.; Niederman, R. A.; Bullough, P. A.; Otto, C.; Hunter, C. N. The native architecture of a photosynthetic membrane. *Nature* **2004**, *430*, 1058.

(3) Griessl, S.; Lackinger, M.; Edelwirth, M.; Hietschold, M.; Heckl, W. M. Self-assembled two-dimensional molecular host-guest architectures from trimesic acid. *Single Mol.* **2002**, *3*, 25.

(4) Theobald, J. A.; Oxtoby, N. S.; Phillips, M. A.; Champness, N. R.; Beton, P. H. Controlling molecular deposition and layer structure with supramolecular surface assemblies. *Nature* **2003**, *424*, 1029.

(5) Wintjes, N.; Bonifazi, D.; Cheng, F.; Kiebele, A.; Stöhr, M.; Jung, T.; Spillmann, H.; Diederich, F. A supramolecular multiposition rotary device. *Angew. Chem., Int. Ed.* **2007**, *46*, 4089.

(6) Elemans, J. A. A. W.; Lei, S.; De Feyter, S. Molecular and supramolecular networks on surfaces: from two-dimensional crystal engineering to reactivity. *Angew. Chem., Int. Ed.* **2009**, *48*, 7298.

(7) Klyatskaya, S.; Klappenberger, F.; Schlickum, U.; Kühne, D.; Marschall, M.; Reichert, J.; Decker, R.; Krenner, W.; Zoppellaro, G.; Brune, H.; et al. Surface-confined self-assembly of di-carbonitrile polyphenyls. *Adv. Funct. Mater.* **2011**, *21*, 1230.

(8) Gopakumar, T. G.; Müller, F.; Hietschold, M. Scanning tunneling microscopy and scanning tunneling spectroscopy studies of planar and nonplanar naphthalocyanines on graphite (0001). Part 1 effect of nonplanarity on the adlayer structure and voltage-induced flipping of nonplanar tin naphthalocyanine. *J. Phys. Chem. B* **2006**, *110*, 6051.

(9) Gottfried, J. M. Surface chemistry of porphyrins and phthalocyanines. *Surf. Sci. Rep.* **2015**, *70*, 259.

(10) Furukawa, S.; Uji-i, H.; Tahara, K.; Ichikawa, T.; Sonoda, M.; De Schryver, F. C.; Tobe, Y.; De Feyter, S. Molecular geometry directed Kagomé and honeycomb networks: toward two-dimensional crystal engineering. *J. Am. Chem. Soc.* **2006**, *128*, 3502−3503.

(11) Arrigoni, C.; Schull, G.; Bléger, D.; Douillard, L.; Fiorini-Debuisschert, C.; Mathevet, F.; Kreher, D.; Attias, A.-J.; Charra, F. Structure and epitaxial registry on graphite of a series of nanoporous self-assembled molecular monolayers. *J. Phys. Chem. Lett.* **2010**, *1*, 190−194.

(12) Tahara, K.; Abraham, M. L.; Igawa, K.; Katayama, K.; Oppel, I. M.; Tobe, Y. Porous molecular networks formed by the self-assembly of positively-charged trigonal building blocks at the liquid/solid interfaces. *Chem. Commun.* **2014**, *50*, 7683.

(13) St. John, A.; Roth, M. W.; Firlej, L.; Kuchta, B.; Charra, F.; Wexler, C. Computer modeling of 2D supramolecular nanoporous monolayers self-assembled on graphite. *Nanoscale* **2019**, *11*, 21284.

(14) Li, B.; Puigmartí-Luis, J.; Jonas, A. M.; Amabilino, D. B.; De Feyter, S. Hierarchical growth of curved organic nanowires upon evaporation induced self-assembly. *Chem. Commun.* **2014**, *50*, 13216.

(15) Wan, L.; Li, L.; Mao, G. Nanospiral formation by droplet drying: one molecule at a time. *Nanoscale Res. Lett.* **2010**, *6*, 49.

(16) Cheng, Z. H.; Gao, L.; Deng, Z. T.; Jiang, N.; Liu, Q.; Shi, D. X.; Du, S. X.; Guo, H. M.; Gao, H.-J. Adsorption behavior of iron phthalocyanine on Au(111) surface at submonolayer coverage. *J. Phys. Chem. C* **2007**, *111*, 9240.

(17) Fendt, L.-A.; Stöhr, M.; Wintjes, N.; Enache, M.; Jung, T.; Diederich, F. Modification of supramolecular binding motifs induced by substrate registry: formation of self-assembled macrocycles and chain-like patterns. *Chem. - Eur. J.* **2009**, *15*, 11139.

(18) Jethwa, S. J.; Kolsbjerg, E. L.; Vadapoo, S. R.; Cramer, J. L.; Lammich, L.; Gothelf, K. V.; Hammer, B.; Linderoth, T. R. Supramolecular corrals on surfaces resulting from aromatic interactions of nonplanar triazoles. *ACS Nano* **2017**, *11*, 8302.

(19) Schenning, A. P. H. J.; Benneker, F. B. G.; Geurts, H. P. M.; Liu, X. Y.; Nolte, R. J. M. Porphyrin wheels. *J. Am. Chem. Soc.* **1996**, *118*, 8549.

(20) Latterini, L.; Blossey, R.; Hofkens, J.; Vanoppen, P.; De Schryver, F. C.; Rowan, A. E.; Nolte, R. J. M. Ring formation in evaporating porphyrin derivative solutions. *Langmuir* **1999**, *15*, 3582.

(21) Lensen, M. C.; Takazawa, K.; Elemans, J. A. A. W.; Jeukens, C. R. L. P. N.; Christianen, P. C. M.; Maan, J. C.; Rowan, A. E.; Nolte, R. J. M. Aided self-assembly of porphyrin nanoaggregates into ring-shaped architectures. *Chem. - Eur. J.* **2004**, *10*, 831.

(22) Saha, P.; Gurunarayanan, V.; Korolkov, V. V.; Vasudev, P. G.; Ramapanicker, R.; Beton, P. H.; Gopakumar, T. G. Selection of adlayer patterns of 1,3-dithia derivatives of ferrocene by the nature of the solvent. *J. Phys. Chem. C* **2018**, *122*, 19067.

(23) Saha, P.; Yadav, V. K.; Gurunarayanan, V.; Ramapanicker, R.; Singh, J. K.; Gopakumar, T. G. Understanding the adsorption energetics of growth polymorphs of ferrocene derivatives: microscopic thermal desorption analysis. *J. Phys. Chem. C* **2019**, *123*, 18488−18494.

(24) Brookhart, M.; Green, M. L. H.; Parkin, G. Agostic interactions in transition metal compounds. *Proc. Natl. Acad. Sci. U. S. A.* **2007**, *104*, 6908.

(25) Bogdanovic, G. A.; Novakovic, S. B. Rigid ferrocene-ferrocene dimer as a common building block in the crystal structures of ferrocene derivatives. *CrystEngComm* **2011**, *13*, 6930.

(26) Pal, R.; Mebs, S.; Shi, M. W.; Jayatilaka, D.; Krzeszczakowska, J. M.; Malaspina, L. A.; Wiecko, M.; Luger, P.; Hesse, M.; Chen, Y.-S.; et al. Linear MgCp*2 vs Bent CaCp*2: london dispersion, ligand-induced charge localizations, and pseudo-pregostic C−H···Ca interactions. *Inorg. Chem.* **2018**, *57*, 4906.

(27) Wedeking, K.; Mu, Z.; Kehr, G.; Fröhlich, R.; Erker, G.; Chi, L.; Fuchs, H. Tetradecyl ferrocene: ordered molecular array of an organometallic amphiphile in the crystal and in a two-dimensional assembled structure on a surface. *Langmuir* **2006**, *22*, 3161.

(28) Wedeking, K.; Mu, Z.; Kehr, G.; Cano Sierra, J.; Mück Lichtenfeld, C.; Grimme, S.; Erker, G.; Fröhlich, R.; Chi, L.; Wang, W.; et al. Oligoethylene chains terminated by ferrocenyl end groups: synthesis, structural properties, and two-dimensional self-assembly on surfaces. *Chem. - Eur. J.* **2006**, *12*, 1618.

(29) Sinnokrot, M. O.; Valeev, E. F.; Sherrill, C. D. Estimates of the ab initio limit for π−π interactions: the benzene dimer. *J. Am. Chem. Soc.* **2002**, *124*, 10887.

(30) Qune, L. F. N. A.; Tamada, K.; Hara, M. Self-assembling properties of 11-ferrocenyl-1-undecanethiol on highly oriented pyrolitic graphite characterized by scanning tunneling microscopy. *e-J. Surf. Sci. Nanotechnol.* **2008**, *6*, 119.